EES Solar

Accepted Manuscript

This article can be cited before page numbers have been issued, to do this please use: J. Luke, S. Chen, Q. He, M. Rimmele, A. V. Marsh, A. J. Gillett, P. Kafourou, Z. Fei, M. Heeney and J. Kim, *EES Sol.*, 2025, DOI: 10.1039/D5EL00166H.

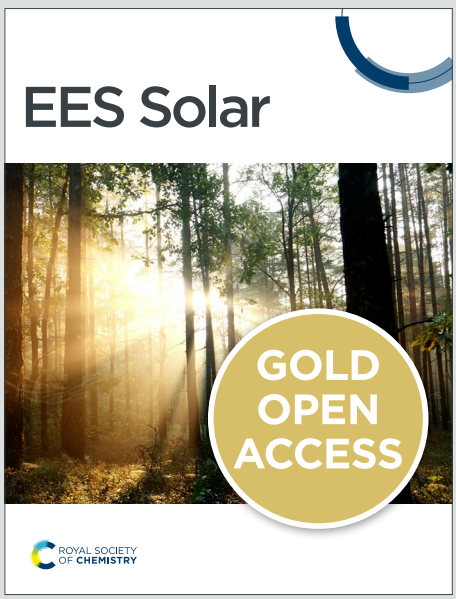

View Article Online
DOI: 10.1039/D5EL00166H

Don’t fluorinate there! The Impact of Fluorination Position on Polymer Photostability and its Effect on Photovoltaic Device Stability

Broader Context Statement: The global energy transition necessitates a rapid shift from fossil fuels to sustainable alternatives. Among these, solar photovoltaics (PVs) have seen remarkable growth driven by the decreasing cost of silicon solar cells. However, the inherent rigidity, opacity, and fixed bandgap of silicon limit its application in niche applications like built-in photovoltaics (BIPVs), agrivoltaics, and indoor energy harvesting. Organic photovoltaics (OPVs) are a promising and versatile alternative due to their tuneable, semi-transparent, and flexible properties, making them ideal for these niche applications. While recent advances have pushed OPV power conversion efficiencies beyond 20%, their operational stability remains a critical challenge, directly impacting their levelized cost of electricity (LCOE) and market competitiveness. In this study, we attempt to improve the stability of a widely used high-performance organic semiconducting polymer by fluorination. We challenge the conventional wisdom that fluorination universally improves ambient photostability by demonstrating a strong dependency of photostability on the fluorine substitution position, with specific fluorination positions leading to severely compromised photostability. This work provides critical insights into the degradation mechanisms of widely used organic semiconductors and establishes new considerations for the molecular design of more stable OPVs.

View Article Online
DOI: 10.1039/D5EL00166H

Don't fluorinate there! The Impact of Fluorination Position on Polymer Photostability and its Effect on Photovoltaic Device Stability

Joel Luke[1,2], Shiyu Chen[1], Qiao He[3], Martina Rimmele[3], Adam V. Marsh[2], Alexander J. Gillett[4], Panagiota Kafourou[2], Fei Zhuping[5], Martin Heeney[2]*, Ji-Seon Kim[1]*

1 Department of Physics and Centre for Processable Electronics, Imperial College London, Blackett Laboratory, London, SW7 2AZ UK

2 Physical Sciences and Engineering Division (PSE), King Abdullah University of Science and Technology (KAUST), Thuwal, 23955–6900 Saudi Arabia

3 Department of Chemistry and Centre for Processable Electronics, Imperial College London, Molecular Sciences Research Hub, White City Campus, London, W12 0BZ UK

4 a) Cavendish Laboratory, University of Cambridge, Cambridge, CB3 0HE UK

b) Department of Physics, Chemistry and Biology (IFM), Linköping University, 581 83 Linköping, Sweden

5 a) Institute of Molecular Plus, Department of Chemistry, Key Laboratory of Organic Integrated Circuits, Ministry of Education &Tianjin Key Laboratory of Molecular Optoelectronic Science, Tianjin University, Tianjin 300072

b) Haihe Laboratory of Sustainable Chemical Transformations, Tianjin 300192, China

Professor Ji-Seon Kim

ji-seon.kim@imperial.ac.uk

Professor Martin Heeney

martin.heeney@kaust.edu.sa

Keywords: organic semiconductor; fluorination; photostability; non-covalent interactions; organic photovoltaic; device stability

View Article Online
DOI: 10.1039/D5EL00166H

Abstract

Despite the excellent progress in organic photovoltaic (OPV) efficiencies, they still suffer from poor operational stability. This is especially true in ambient conditions, with degradation often driven by intrinsic material instabilities. Fluorination of the constituent organic semiconductors, which deepens frontier orbitals and improves organic semiconducting packing, is often utilised to improve photostability. Here, fluorinated analogues of the high-performance workhorse polymer PBDB-T are synthesised and their photostability characterised. Device stability, with both Y6 and IT-4F, is found to be critically dependent on the intrinsic polymer photostability, with fluorination of the benzodithiophene (BDT) being particularly ruinous for stability. The carbonyl group in these unstable BDT-fluorinated analogues is found to be highly unstable towards illumination. This instability arises from a disruption of non-covalent interactions along the polymer backbone, where the fluorine on BDT interferes with intramolecular S-O interactions between the thiophene and benzodithiophene-dione (BDD) carbonyl. This leads to increased backbone disorder and a more vulnerable carbonyl environment. These results challenge the conventional belief that fluorination universally improves OPV stability and underscore the crucial role of non-covalent interactions in governing material stability.

View Article Online
DOI: 10.1039/D5EL00166H

Introduction

Organic photovoltaics (OPVs) continue to improve in efficiency, now achieving > 20% in single-junction cells.(1-3) Despite this, the poor longevity of OPVs remains a considerable barrier towards commercialisation.(4, 5) Given the multilayered structure of OPV devices, degradation within any layer or interface is possible.(6) However, the most critical factor for determining device stability is often the photoactive organic layer due to its sensitivity to illumination, particularly in ambient atmospheres.(7-10) Encapsulation mitigates degradation by inhibiting air ingress, yet it only slows the process, highlighting the need for intrinsically stable organic semiconductors (OSCs).(11, 12)

One potential strategy that we have suggested as a design rule for improving the stability of OSCs is fluorination.(4) Fluorination is known to deepen a molecule's frontier molecular orbital energy levels, improving the OSC's ambient stability.(13-15) Non-covalent fluorine-sulfur interactions are also known to planarise conjugated backbones,(16-19) potentially inhibiting any conformational changes upon degradation.(7) Fluorination has also been demonstrated to enhance the molecular quadrupole, which is increasingly being used to improve device performance(20) and photostability.(8) Additionally, fluorination often improves the solid-state packing of OSCs, reducing π-π stacking distances and enhancing crystallinity, improving the OSC's morphological and photo-stability.(21-24)

While the PBDB-T class of donor polymers,(25, 26) particularly PM6,(27) have become OPV workhorses due to their excellent efficiencies when paired with the Y-series of acceptors,(27) recent studies have identified the instability of this class of polymers toward ambient illumination. Under illumination in ambient air, we observed a twisting of the polymer backbone, resulting in ultrafast polaron pair formation, which acts as an exciton trap, inhibiting charge transfer and driving device degradation.(9) This degradation mechanism was isolated to the electron-rich benzodithiophene unit, suggesting its use may be problematic in the search for stable OSCs. This has been confirmed by further studies by Prasad *et al.,* who found that the inclusion of the BDT-T linker in Y-series acceptor polymers led to poor ambient photostability.(28)

In this study, we investigate the impact of PBDB-T fluorination position on polymer stability to understand if the fluorination strategy can be used to improve the photostability of this important class of polymers. PBDB-T is a donor-acceptor copolymer comprised of an electron-rich benzodithiophene (BDT) and an electron-deficient benzodithiophene-dione (BDD) separated by thiophene (T) linkers. Solubilising sidechains of 2-(2-ethylhexyl) thiophene and 2-ethylhexyl are attached to the BDT and BDD units, respectively. We compare the stability of five polymers (chemical structures in Figure 1) with different

View Article Online
DOI: 10.1039/D5EL00166H

positions of fluorination: PBDB-T (no fluorine), PM6 (thiophene sidechain fluorination), PT-2F (thiophene spacer fluorination, previously named PFBDB-T),(29) PBDT-2F (BDT unit thiophene ring fluorination),and PTDBT-4F (BDT and thiophene linker fluorination).(30) We find fluorination of the thiophene spacers to mildly improve device stability. Interestingly, however, fluorination of the BDT unit itself is disastrous for polymer stability. These findings demonstrate fluorination's potential for improving OPV stability but highlight how sensitive this effect is towards the position of fluorination.

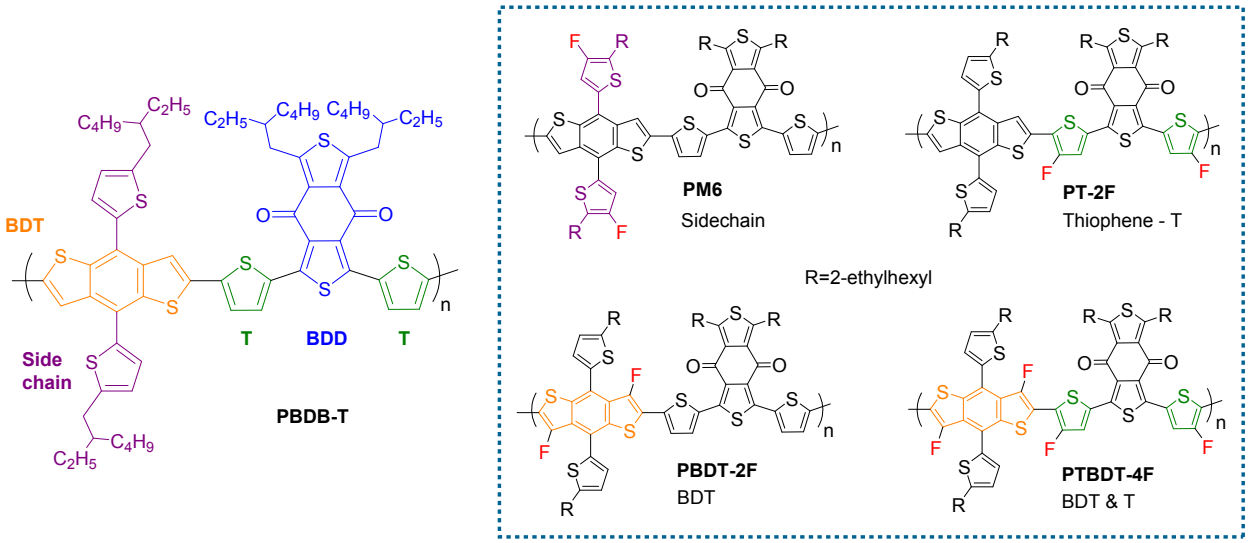

Figure 1. Chemical structures of the PBDB-T class of polymers studied here with different fluorination positions.

Results and Discussion

Polymer Properties

PBDB-T and PM6 were sourced from commercial sources (see Methods), whilst the fluorinated analogues PT-2F, and PTBDT-4F were synthesised using our previously reported procedures.(29, 30) The synthesis of the previously unreported PBDT-2F is given in the Supporting Information (Figure S1). The basic properties of the polymers are summarised in Table 1.

The number average molecular weights (M_n) of the polymers were assessed with high temperature (150°C) gel permeation chromatography (GPC) to avoid aggregation effects. All polymers were in the M_n range of 35-69 kDa and with dispersities (Đ) between 2-3.3. Whilst molecular weight is known to impact device performance, these values are within the range previously shown to give consistent device performance for PBDB-T and PM6, i.e. neither very high nor very low.(31, 32) Since all polymers have a

View Article Online
DOI: 10.1039/D5EL00166H

sufficiently large M_n to be above the effective conjugation length, we believe we can reasonably compare between polymer batches.

The neat polymer film absorption spectra (Figure S3) show that fluorination along the conjugated backbone slightly narrows the band gap. The lowest energy absorption peak in these polymers correlates to aggregated polymer, as determined by temperature-dependent absorption measurements on solvated PBDB-T.(33) This peak shifts 10-20 nm to longer wavelengths for PT-2F and PTBDT-4F, indicating thiophene fluorination encourages polymer aggregation. Air photoemission spectroscopy (APS) gives the ionisation energy of the polymers (Figure S4), which is commonly equated with the highest-occupied molecular orbital (HOMO) energy level.(34, 35) Fluorination deepens the HOMO level in all cases, the details of which are discussed below.

Table 1. *An overview of the basic properties of the polymers studied herein. Absorption max ($\lambda_{max,film}$) and optical band gaps ($E_{g,opt,\ film}$) are extracted from the UV/vis absorption spectra, ionisation energies (IE_{APS}) are extracted from air photoemission spectroscopy (APS), with the LUMO estimated by addition of the IE_{APS} with the $E_{g,opt,film}$. The number-average molecular weight (Mn) is given along with the polydispersity index (Đ).*

Polymer	$\lambda_{max,film}$ / nm	$E_{g,opt,\ film}$ / eV	IE_{APS} / eV	LUMO (IE_{APS} + $E_{g,opt,film}$) / eV	M_n / kDa	Đ
PBDB-T	614	1.85	-4.87	-3.02	65	2.3
PM6	618	1.84	-5.06	-3.22	36	2.7
PT-2F	640	1.80	-4.92	-3.12	50	2.0
PBDT-2F	616	1.82	-5.10	-3.28	69	3.3
PTBDT-4F	630	1.80	-5.15	-3.35	47	2.1

Polymer Photostability

To investigate the photostability of our polymers, we studied neat and blend films before and after 24 hours of photodegradation in air (Figure S3) with the absorption spectra of PT-2F and PT-2F:Y6 films shown in Figure 2. The absorption percentage remaining after degradation of all the polymers is compared in Figure 2c. Upon ageing, the main absorption peak of PT-2F is bleached, with a more pronounced quenching of the low-energy aggregation peak (as determined from previous temperature-dependent studies)(36) and an increase in sub-gap absorption, indicating disrupted polymer packing, more disorder and the emergence of sub-gap states in the degraded polymer. PBDB-T and PM6 also show these features

View Article Online
DOI: 10.1039/D5EL00166H

with a similar amount of quenching; however, PT-2F maintains a more pronounced aggregation peak following degradation. Surprisingly, within 24 hours, the absorption peaks of PBDT-2F and PTBDT-4F are nearly entirely bleached. Even after 2 hours of ageing (Figure S3), the films bleach significantly more than the 24 hour degraded films of the other polymer. Such rapid absorption bleaching reveals a severe instability of these two polymers towards illumination in air. Further, blend film studies (Figure S7) reveal similar polymer absorption bleaching with a similar trend to the neat films, with PBDT-2F and PTBDT-4F being the most unstable. The acceptor absorption is also bleached, but to a lesser extent, suggesting that the polymer is the crucial component determining blend stability.

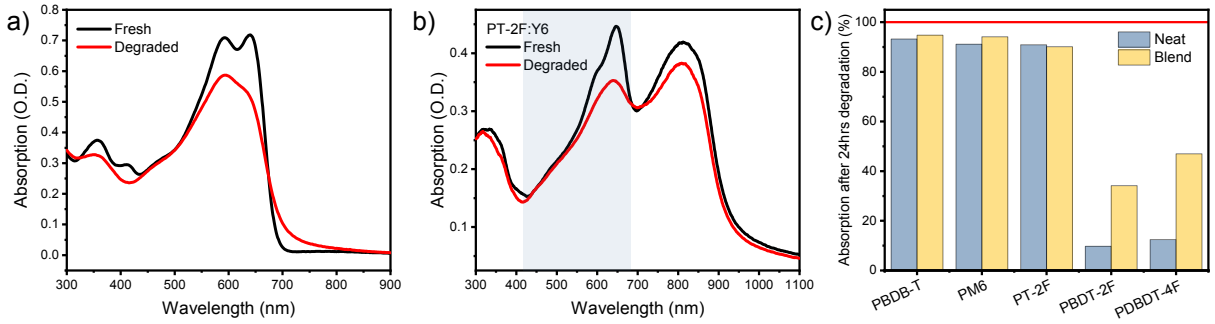

Figure 2. Film absorption spectra of neat PT-2F (a) and PT-2F blends with Y6 (b) before and after 24 hours of 1 sun illumination in ambient air; (c) the integrated absorption of all neat polymer and Y6-blend films after degradation relative to the fresh absorption; for blend films the blue-shaded area in (b) shows the wavelength range used for integration of the specific polymer absorption.

Impact on Device Stability

To understand how this polymer instability translates to devices, inverted ITO/ZnO/Polymer:Acceptor/MoO_X/Ag solar cells were fabricated with the common acceptors Y6 and IT-4F, which were chosen for their high performance and demonstrated photostability in devices. Device performances are given in Figure S5. It should be noted that the devices used were not optimised for efficiency, as we wanted to avoid thermal annealing and the use of additives to isolate the effect of polymer selection. As such, the efficiencies are lower than those of similar devices in the literature. With IT-4F, all fluorinated polymers give more efficient devices than PBDB-T, demonstrating enhanced open-circuit voltage (V_{OC}) and fill factor (FF). While only the PT-2F devices perform superior to the nonfluorinated polymer when paired with Y6, despite a higher V_{OC} being achieved with all the fluorinated polymers.

View Article Online
DOI: 10.1039/D5EL00166H

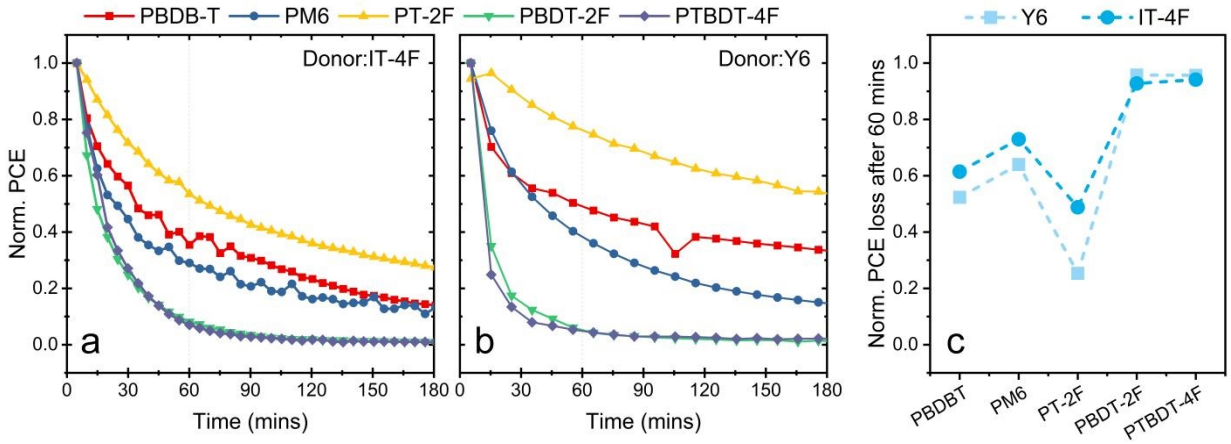

Figure 3. Device stability of the PBDB-T class of polymers. (a & b) Average, normalised power conversion efficiencies (PCE) of ITO/ZnO/Donor:Acceptor/MoO_3/Ag devices as a function of illumination time in air; (c) normalised PCE loss of these devices after 60 minutes ageing.

These devices were degraded at open circuit under ambient conditions with a white LED at 1 sun light intensity, calibrated by device current matching. The evolution of power conversion efficiency with illumination time is shown in Figure 3, with full device parameters shown in Figure S6. Both sets of devices degrade rapidly in air, predominantly driven by a loss of J_{SC}, consistent with our previous reports on PBDB-T and PM6 degradation.(9) The Y6 devices with PBDB-T, PM6, and PT-2F have superior stability to their IT-4F counterparts. With both acceptors, PT-2F devices are the most stable, followed by PBDB-T and PM6, which show similar lifetimes. The unstable polymers PBDT-2F and PTBDT-4F show the worst device stability, losing nearly all efficiency within 30 minutes of degradation, highlighting the key role of polymer stability in determining the overall device stability. The PCE loss of the different polymer devices after one hour of degradation is compared in Figure 3c.

Nature of Degradation

As in our previous study, we employ transient absorption spectroscopy after 2 hours of film degradation to understand the nature of degradation in the BDT-fluorinated polymers (Figure S8, Figure S9). For all fresh polymers, we observe a ground state bleach (GSB) around 600 nm, stimulated emission (SE) 700-750 nm, a broad photoinduced absorption (PIA) centred around 1000 nm assigned to the S_1 state, and a small shoulder feature at 900 nm related to the polymer polaronic absorption, which overlaps with the S_1 PIA. After ageing, PBDB-T and PM6 show a quenched SE band and an enhanced photoinduced absorption (PIA) signal at 900 nm within the first couple of picoseconds, consistent with ultrafast polaron pair formation.(9) Both these signatures are more subtle for PT-2F, indicating enhanced stability towards the

View Article Online
DOI: 10.1039/D5EL00166H

detrimental formation of trapped polaron pairs. Similarly, upon ageing, PBDT-2F and PTBDT-4F show SE quenching and an increase in the polaron signal at 900 nm. However, at 1-2 ps, the PIA intensity increases relative to the GSB nearly 3 times compared to PT-2F and is also accompanied by a change in the PIA shape. Furthermore, consistent with the steady state absorption measurements, the GSB for PBDT-2F and PTBDT-4F shows a noticeable blue shift and a near-complete loss of vibronic features. Thus, the TAS data suggest that an additional photophysical process is occurring following degradation of these two polymers.

The common feature distinguishing PBDT-2F and PTBDT-4F from the other polymers is the fluorination of the BDT unit, which appears to be disastrous for polymer photostability. This has previously been seen in a series of thienothiophene polymers containing fluorinated BDT units.(23) In that study, the accelerated degradation of BDT-fluorinated polymers was assigned to accelerated singlet oxygen [2+4] cycloaddition due to differences in internal polarisation. Below, we present energetic, chemical, and computational analyses to investigate potential degradation mechanisms in our polymer series.

Generally, illumination in air is thought to initiate photooxidation in OSCs. Photooxidative stability has been correlated to the energy levels of a material, with deeper frontier energy levels corresponding to enhanced stability.(37) The highest-occupied-molecular-orbital (HOMO) energy levels of the polymers, measured by air photoemission spectroscopy (APS) before and after ageing, are shown in Figure 4. The HOMO levels of the fresh polymer films are -4.87, -4.92, -5.06, -5.10, and -5.15 eV for PBDB-T, PT-2F, PM6, PBDT-2F, and PTBDT-4F, respectively. Due to the electronegativity of fluorine, fluorination results in a deepening of HOMO energy levels, with the magnitude of this depending on the number and position of fluorine atoms. We can see that the fluorination on the BDT unit, either on the sidechains as in PM6 or on the main conjugated backbone, results in the strongest stabilising effect, deepening the HOMO by ~0.2 eV. In comparison, thiophene fluorination only deepens the HOMO level by 0.05 eV. This is understood in terms of the D-A structure of the polymer, where the wavefunction of the HOMO is predominantly localised on the electron-rich donor BDT unit. As such, direct modification of this unit will result in a more substantial effect on the HOMO energy. With the band gap of the polymers being similar, the LUMO levels follow the HOMO trend. Surprisingly, the deeper energy levels of the BDT fluorinated polymers do not confer improved ambient photostability.

View Article Online
DOI: 10.1039/D5EL00166H

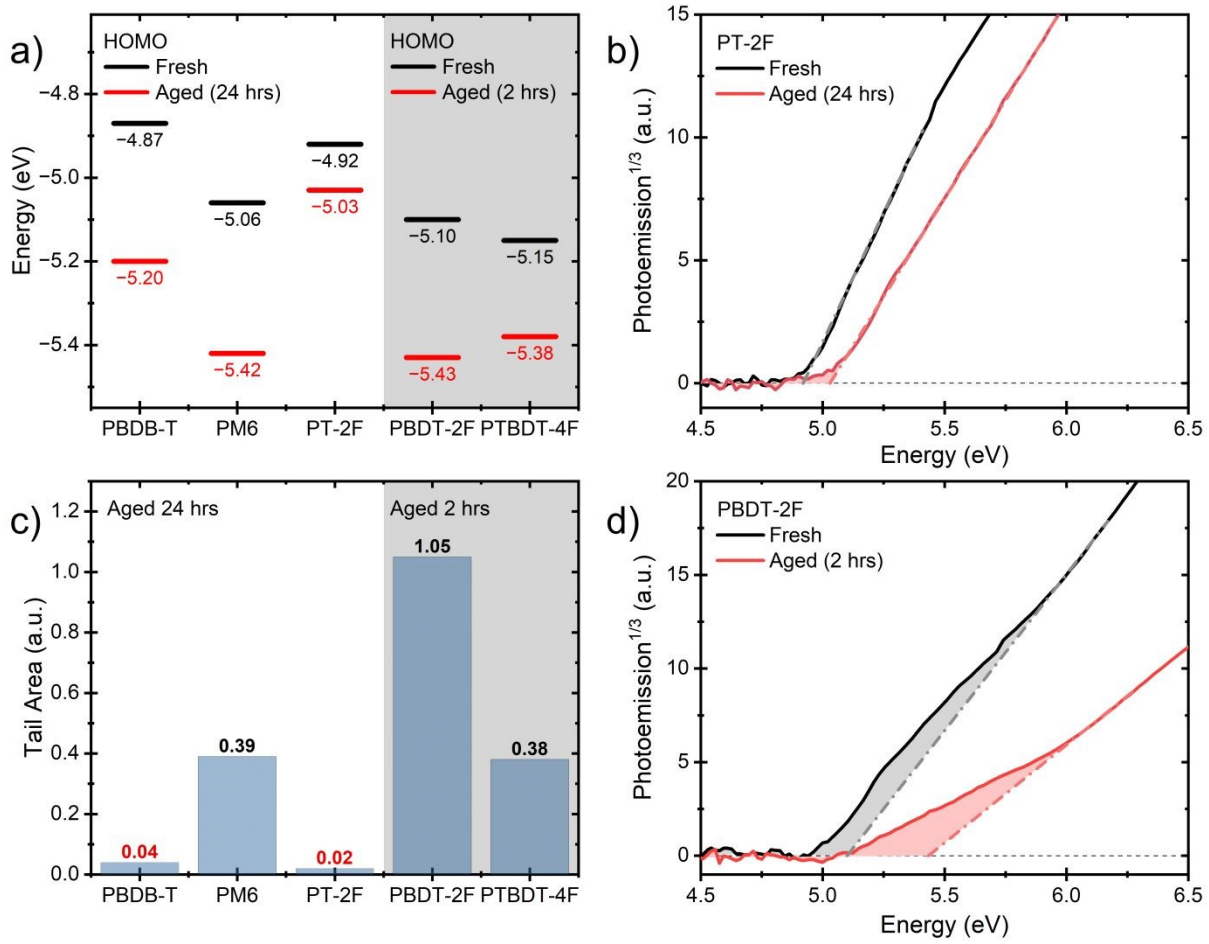

Figure 4. Energetics of the PBDB-T series of polymers. (a) the air photoemission spectroscopy (APS) derived HOMO levels of the polymers before and after ageing; (b)+(d) are examples of the APS spectra obtained for the PT-2F and PBDT-2F polymers, with their tail area shaded; (c) extracted APS tail areas of polymer films after ageing.

Following 24 hours of ageing, the HOMO levels of PBDB-T and PM6 are deepened by roughly the same energy ~0.35 eV, whilst PT-2F deepens by only 0.11 eV. After 24 hours, the HOMO levels of PBDT-2F and PTBDT-4F cannot be measured using APS. Still, after 2 hours of ageing, a deepening of 0.33 and 0.18 eV is observed, again showing their relative instability compared to the other polymers. APS is a surface-sensitive technique, so in degraded films, it is particularly sensitive to the most degraded material, i.e. the first few nanometres exposed to air. The disrupted conjugation in the degraded polymers widens the bandgap, deepening the HOMO level. In addition to giving the HOMO energy, the tail area of the APS measurements gives an idea about the energetic disorder around the HOMO.(38, 39) The tail areas of fresh and aged films are visible in Figure S4, with extracted values of the aged films summarised in Figure 4c. Fresh polymer films show that PBDB-T, PM6, and PT-2F have smaller tail areas than PBDT-2F and

View Article Online
DOI: 10.1039/D5EL00166H

PTBDT-4F, indicating that the fresh unstable polymers are more energetically disordered. After ageing, the tail area increases, indicating higher energetic disorder in the degraded polymers. This area is still small for PBDB-T and PT-2F, slightly larger for PM6, and largest for PBDT-2F and PTBDT-4F, even after only 2 hours of ageing. The deepening of the HOMO energy level and increasing disorder are consistent with UPS studies on fresh and degraded PBDB-T presented elsewhere.(28)

PT-2F shows the least change in energetics, with the HOMO only shifting by 0.11 eV. PT-2F also maintains the highest relative intensity of the aggregation absorption peak. The more stable aggregation state of PT-2F can explain the relative energetic stability, as the most aggregated polymer will have the lowest bandgap and define the HOMO level in the film. AFM images of the more stable polymer films show fibril structures, which are finer for PT-2F than PBDB-T and PM6 (Figure S10). The improved energetic stability and finer morphology may account for the enhanced device stability of PT-2F relative to PBDB-T and PM6, as the finer fibril structure forms a more stable morphology with the acceptor. Photostability is also improved by minor improvements in crystallinity, and therefore, small changes in the polymer or blend morphology may impact photostability.(40) We also note that PBDT-2F and PTBDT-4F films have less pronounced fibril structure, with this less ordered morphology accounting for the greater energetic disorder observed in these films.

Molecular Origin of Photodegradation

To understand the molecular origin of polymer degradation in more detail, we used *in situ* Raman spectroscopy with a resonant degradation and probe laser at 514 nm (Figure S11). Raman peak assignment is consistent with our previously reported assignment of PBDB-T.(9) Following extended laser illumination, the Raman intensity of all the polymers is reduced. When normalised, relative peak intensity changes become apparent. For all the polymers, we see changes consistent with those previously assigned to the photoinduced twisting of the conjugated backbone away from planarity.(9) This is consistent with the TAS data above, which shows polaron pair formation in PBDB-T, PM6, and PT-2F. However, this does not explain the relative instability of the BDT-fluorinated polymers, nor does it reveal an additional degradation mechanism as suggested by the TAS data.

Instead, we turn to FTIR analysis to investigate the products of degradation. The FTIR spectra of fresh and degraded PT-2F and PBDT-2F are shown in Figure 5a to represent the stable and unstable polymers, with other polymers shown in Figure S12-15. After 1 hour of 1 sun illumination in air, the PT-2F is relatively stable, showing only a small reduction in the carbonyl peak at 1648 cm^{-1}, assigned to the BDD unit and the

View Article Online
DOI: 10.1039/D5EL00166H

growth of a new, broad peak at 1705 cm^{-1}, likely associated with C=O. Differently, PBDT-2F shows a significant reduction in the carbonyl peak, a greater increase of the peak around 1705 cm^{-1}, another possible new carbonyl peak at 1833 cm^{-1}, a new peak at 1190 cm^{-1}, and changes in the C=C fingerprint region. We note that no new broad peaks at higher frequencies (ca. 3300 cm^{-1}, Figure S15) in the degradation product indicate the presence of OH bonds. The significant loss of the BDD carbonyl peak in the unstable polymers indicates that this is the key instability driving the rapid degradation of these polymers.

The broad degraded product peak at 1705 cm^{-1}, observed across all polymers, which we attribute to new carbonyl (C=O) stretching vibrations, is consistent with X-ray photoelectron spectroscopy (XPS) studies on PBDB-T that show photooxidation of carbon.(28, 41) We note that these studies also indicate direct photooxidation of sulfur at longer degradation times, although this is not apparent in our FTIR analysis. For the more unstable BDT-fluorinated polymers, the additional degraded peaks indicate a new degradation product. The band at 1833 cm^{-1} is unusually high in frequency for a typical carbonyl stretch but may be attributed to an acid anhydride. The anhydride (O=C-O-C=O) is expected to result in two carbonyl peaks due to the symmetric and asymmetric stretches of the two carbonyl groups, with the lower energy symmetric peak being found within the broad carbonyl band around 1705 cm^{-1}. The new absorption at 1190 cm^{-1} could also correspond to the C-O-C stretching mode of an acid anhydride. Alternatively, the high-frequency carbonyl could be the result of an acyl fluoride, and the peak at 1190 cm^{-1} resulting from a sulfone (S=O) stretch vibration. In any case, the new photooxidation product results in a disruption of the conjugated backbone, as demonstrated by the changes in the FTIR C=C fingerprint region, and consistent with rapid optical absorption loss and widening bandgap observed above.

Despite not pinpointing the exact degradation product, we have outlined a distinct conjugation-breaking product in the unstable BDT-fluorinated polymers originating from a new degradation pathway. We discuss the origin of this degradation pathway below.

View Article Online
DOI: 10.1039/D5EL00166H

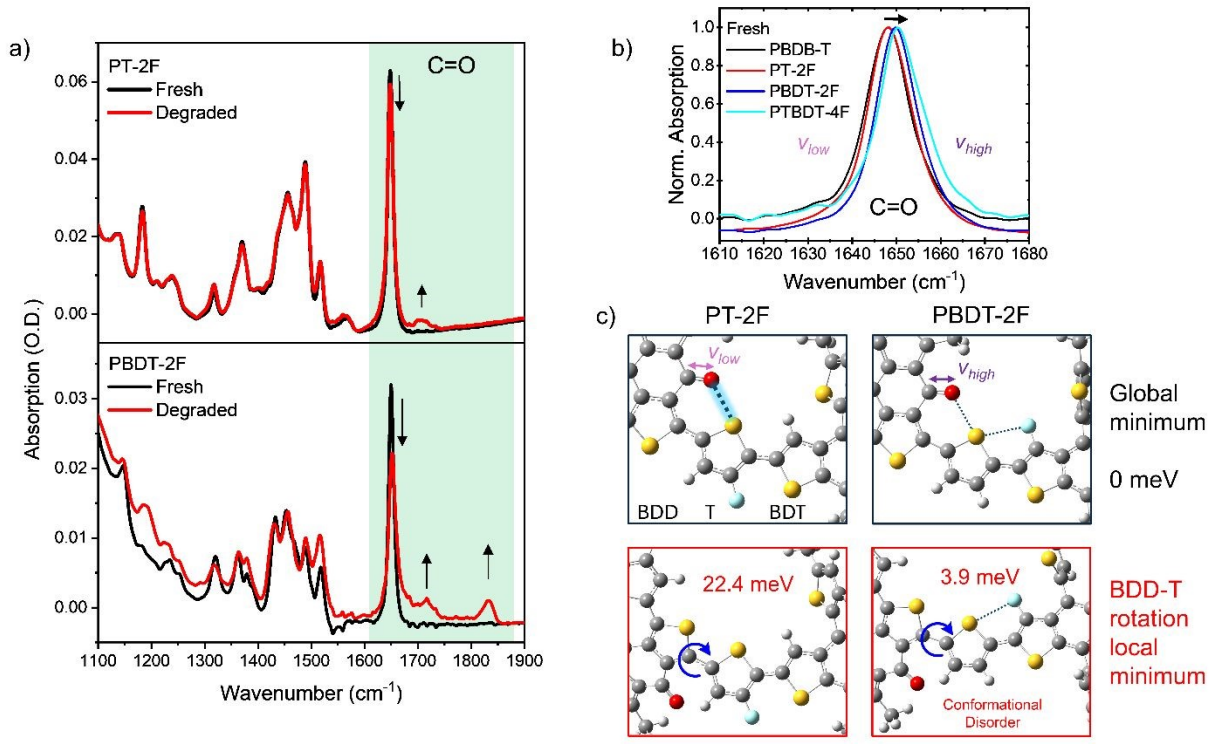

Figure 5. Chemical Degradation Analysis. (a) FTIR spectra of PT-2F and PBDT-2F films on CaF substrates before and after 1 hour of 1 sun illumination in air; (b) FTIR spectra of fresh polymer films normalised to the carbonyl peak; (c) A segment of the energy minimised structure (top) of PT-2F (left) and PBDT-2F (right) with intramolecular non-covalent interactions between the thiophene sulfur and both the BDD carbonyl and BDT fluorine highlighted with dashed lines. The same polymers (bottom) after BDD-T dihedral rotation to a localised energetic minimum, energies of which are given relative to the global minimum energy structure.

As an observed weak point, we investigate the nature of the carbonyl bonds in the polymer series by plotting the normalised IR carbonyl peak of the fresh polymers in Figure 5b. The carbonyl peak is shifted to higher frequencies in the BDT-fluorinated polymers, indicating a stronger carbonyl bond. We rationalise this by considering potential non-covalent interactions along the polymer chain. The sulfur in the thiophene spacer unit forms attractive non-covalent interactions with the BDD carbonyl oxygen, driven by electrostatic and dipole interactions.(16) Similarly, S-F electrostatic interactions are possible, although these are weaker than S-O interactions.(16) Nevertheless, with BDT fluorination, the sulfur on the spacer thiophene can form non-covalent interactions with the fluorine on BDT in addition to the S-O interactions with BDD. The competing S-F interaction weakens the S-O interaction, resulting in the stronger carbonyl bond observed with FTIR. The top panels of Figure 5c depict these interactions as dotted lines, with thickness indicating interaction strength, for the stable PT-2F and unstable PBDT-2F polymers. We postulate that the S-O interaction stabilises the polymer during photophysical degradation processes,

View Article Online
DOI: 10.1039/D5EL00166H

stabilising the polymer conformation and structure. When this interaction is weakened, the polymer becomes more unstable, demonstrating the critical role that molecular structure plays in determining polymer photostability.

Simulations

DFT simulations were performed using Gaussian16 to confirm the impact of BDT-fluorination on the carbonyl group and to investigate the degradation mechanism further.(42) The B3LYP-D3 functional and 6-311G(d,p)++ basis set were utilised to model diffuse orbitals and dispersion effects, which are critical for modelling non-covalent interactions.(43-45) Molecular orbital diagrams on polymer trimers are shown in Figure S16. HOMOs are delocalised across the conjugated backbone in C=C bonds, while the LUMO is more localised to the BDD-T unit, with fluorination leading to small changes in the degree of LUMO localisation to the BDD unit.

Partial atomic charges are calculated using the electrostatic potential (ESP) method ChelpG, which gives the electrostatic potential on each atom and has been shown to give more consistent results between different basis sets.(16, 46) Electrostatic potential surfaces of the polymer monomers are shown in Figure S17, with localised areas of negative potential concentrated around the electronegative fluorine atoms. The extracted carbonyl oxygen atomic charges are -0.405, -0.404, -0.396 for PBDB-T, PM6, PT-2F, while BDT-fluorination reduces the partial charge of PBDT-2F and PTBDT-4F to -0.385, and -0.377. The reduced oxygen charge is indicative of a weakened S-O interaction, highlighting the key impact of BDT-fluorination.

The impact of the S-O interaction on polymer conformation is explored through dihedral energy scans of the BDT-T and BDD-T interunit bonds (Figure S18). It has been previously shown that the degradation of PM6 can be related to the twisting of the conjugated backbone about these interunit bonds.(9) In the lowest energy conformations of all the polymers, the sulfur of BDT and the thiophene spacer face opposite directions (anti). Fluorination along the backbone planarises the BDT-T linkage with dihedral angles given in Figure S19. A second local energetic minimum is observed when the BDT-T dihedral angle is again close to planarity, but with the sulfur atoms being syn. The energy of these local minima depends on the polymer, with a detailed explanation outlined in Figure S18. PBDB-T and PTBDT-4F have relatively high local minima (60 meV), while PT-2F and PBDT-2F have local minima only 15-18 meV above the global minima. These energetic differences show no correlation with the polymer stability trend observed and, therefore, cannot explain the degradation mechanism of BDT-fluorinated polymers.

View Article Online
DOI: 10.1039/D5EL00166H

Now, focusing on the BDD-T dihedral, we expect the S-O interactions to play a more critical role. Rotation about this dihedral is shown in Figure 5c for PT-2F and PBDT-2F. The minimum energy structure (Figure 5c, top panels) in all polymers is when the sulfur of the thiophene spacer and carbonyl of BDD are on the same side, with a dihedral angle of ~15°. Rotation about the BDD-T dihedral by ~180° results in a second local minimum when the spacer thiophene sulfur and BDD carbonyl are anti (Figure 5c, bottom panels). For PBDB-T and PT-2F these minima are 20 meV higher in energy than the global minimum, demonstrating the stabilising effect of the S-O interaction when the sulfur and carbonyl are syn. In the BDT-fluorinated polymers, the barrier to BDD-T rotation is lower, and the local anti-minima are <5 meV above the global minimum, demonstrating weaker S-O stabilisation. The lower rotation barrier and energetic similarity between the syn and anti-conformers in the BDT-fluorinated polymers will result in conformational and structural disorder in the polymer. This is consistent with the increased energetic disorder of the BDT-fluorinated polymers as measured by APS and the less pronounced fibril structure in AFM images. It also highlights the impact of BDT-fluorination on weakening the S-O non-covalent interaction, corroborating our experimental evidence that BDT-fluorination affects the BDD carbonyl.

Sidechain-driven degradation has been demonstrated to be a key degradation pathway through both photooxidation(41) and photophysical processes such as homolytic fission of C-C bonds and H abstraction.(47) The likelihood of these photophysical processes occurring can be interrogated by calculating the Laplacian bond order (LBO) of the labile bonds, which we detail for our polymer series in Figure S20 and Figure S21.(47, 48) All polymers show similar LBOs for all the bonds considered, indicating that the differences in sidechain stability cannot account for the dramatic differences we observe in photostability. Considering photooxidation, XPS analysis has suggested that PBDB-T undergoes alkyl-sidechain photooxidation.(41) However, the pronounced loss of conjugation observed in the absorption spectra and energetic degradation of the unstable BDT-fluorinated polymers, together with the C=C peak changes in the FTIR spectra, indicate that photooxidation is more probably occurring on the conjugated backbone.

Photooxidation can proceed via the photoinduced formation of reactive oxygen species, such as superoxide or singlet oxygen.(14) Superoxide can be formed following photoinduced electron transfer from the LUMO of an OSC to molecular oxygen. The single reduction potential of O_2 is -4.11 eV,(49) meaning superoxide formation following electron transfer from the LUMO of any of the polymers is thermodynamically favourable and cannot be used to rationalise the observed stability trend.

View Article Online
DOI: 10.1039/D5EL00166H

Singlet oxygen formation occurs via energy transfer from triplet states in the OSC. Once formed, singlet oxygen acts as an electrophile, attacking the electron-rich conjugated backbone through cycloaddition reactions. A [2+2] cycloaddition of the BDT thiophene ring has been proposed as a degradation pathway in PBDB-T.(50) In the present case, however, fluorination is expected to deactivate the BDT thiophene towards such electrophilic attack. Beyond the substituted ring, fluorination impacts the electron distribution along the conjugated backbone and may influence the reactivity of other units towards singlet-oxygen attack. A previous study employing partial charge analysis reported that fluorination of the BDT unit accelerates singlet oxygen [2+4] cycloaddition of the thienothiophene co-monomer due to an increase in local electron density.(23) We performed an equivalent analysis of our polymer series using the ChelpG method introduced above (Figure S22). The analysis focused on the electro-negativity of the α-carbons on the BDT thiophene ring, the thiophene linker, and the thiophene of BDD unit, identified as potential sites for [2+4] cycloaddition. In fluorinated polymers, the α-carbon closest to the fluorination site becomes more electron-rich; however, the impact on adjacent thiophene rings is less systematic, showing no clear correlation with the observed stability trend. These results indicate that the initial reactivity towards singlet oxygen alone cannot account for the differences in stability we observe.

To shine further light on the degradation mechanism, we investigated the impact of the atmosphere on photodegradation. Here, polymer films were illuminated in an inert N_2 atmosphere, and their absorption spectra were measured (Figure S23). After 24 hrs illumination, PBDB-T, PM6, and PT-2F absorption showed minimal changes, while PBDT-2F and PTBDT-4F demonstrated clear bleaching, albeit at a slower rate than photodegradation in air. This suggests that the instability of the BDT-fluorinated polymers is an intrinsic instability to illumination, which is accelerated by oxygen. Although this does not exclude the possibility of a singlet oxygen attack, it suggests an instability within the polymer itself. Based on this, we postulate that a photophysical change along the conjugated backbone is an important degradation mechanism. This change could be a photo-induced ring-opening,(51) a photoisomerisation,(52) or bond scission; we discuss these possibilities in more detail in Supplementary Note 1. The S-O non-covalent interaction then provides a scaffolding for the molecular conformation and structure, either resisting initial photophysical changes or facilitating the reformation of the ground-state polymer structure without further reactions or conjugation loss. When this interaction is weakened by competing S-F interactions, the initial photophysical change is more likely to be followed by further irreversible chemical changes, either through isomeric reorganisation or interactions with external species, resulting in new degradation products and a loss of backbone conjugation.

View Article Online
DOI: 10.1039/D5EL00166H

Conclusion

Our data suggests that BDT-fluorination severely compromises the photostability of PBDB-T polymers, which is critical for device photostability. Upon degradation BDT-fluorinated polymers exhibit an additional degradation mechanism centred on the carbonyl bonds in the BDD unit. We have provided experimental evidence of a different C=O environment in BDT-fluorinated polymers. Through a combination of simulations, we assign this to the disruption of the intramolecular S-O non-covalent interaction between thiophene and BDD by competing S-F interactions between the thiophene and BDT in BDT-fluorinated polymers. Weakening the S-O interaction results in more backbone structural disorder and a propensity to conjugation loss upon illumination. We hypothesise that weakening the intramolecular S-O non-covalent interactions makes the polymer more prone to irreversible photophysical changes. Strong S-O interactions act as a structural scaffold, inhibiting photophysical changes such as isomerisation or facilitating reformation of the initial structure following, say, photoinduced ring-opening. Without this stabilising template, the ring-opening process leads to further irreversible reactions, such as isomerisation or reactions with environmental species.

In general, the role of these non-covalent interactions is challenging to decipher due to the lack of direct experimental techniques, the various computational methods available, and the inherent energetic and structural disorder in organic semiconducting polymers. Further work in this area is required to develop tools to characterise these non-covalent interactions and apply these to the applied challenges in organic semiconductors.

Our results highlight the impact of fluorination position on polymer photostability, challenging the general assumption that fluorination always enhances stability through improved packing and deeper energy levels. We demonstrate that the key non-covalent interactions in fluorinated PBDB-T polymers are not S-F interactions but rather S-O interactions between the thiophene and BDD. Destabilising these S-O interactions can severely compromise photostability, highlighting a crucial molecular design rule when utilising the commonly employed BDD unit. More generally, the fluorination position should be chosen to avoid disrupting planarizing non-covalent interactions. Fluorination, therefore, is not a one-size-fits-all solution for improving polymer stability, as it can influence other intermolecular interactions along the polymer backbone. We do not want to discourage the use of fluorination to improve efficiency, but emphasise that new OPV materials, particularly fluorinated analogues, should be screened for photostability through basic photobleaching experiments.

View Article Online
DOI: 10.1039/D5EL00166H

Acknowledgements:

The authors would like to acknowledge the UK Engineering and Physical Sciences Research Council for funding through both the Application Targeted and Integrated Photovoltaics programme grant (EP/T028513/1) and the Centre for Doctoral Training in Plastic Electronic Materials (EP/L016702/1). Additionally, J.L, A.V.P, P.K. and M.H. thank the King Abdullah University of Science and Technology (KAUST) under award (ORFA-CRG11-2022-5045). A.J.G. thanks the Leverhulme Trust for an Early Career Fellowship (ECF-2022-445), the Knut and Alice Wallenberg Foundation for a Wallenberg Academy Fellows award (KAW 2023.0082), and the Swedish Research Council (VR) for a Starting Grant (2024-03915).

Conflict of Interest

The authors declare no conflicts of interest.

References

1. Zhu L, Zhang M, Zhou Z, Zhong W, Hao T, Xu S, et al. Progress of organic photovoltaics towards 20% efficiency. Nature Reviews Electrical Engineering. 2024;1(9):581-96.
2. Wei N, Chen J, Cheng Y, Bian Z, Liu W, Song H, et al. Constructing Multiscale Fibrous Morphology to Achieve 20% Efficiency Organic Solar Cells by Mixing High and Low Molecular Weight D18. Adv Mater. 2024;36(41):e2408934.
3. Du M, Sun N, Cheng H, Liu X, Yi X, Guo Q, et al. Multiple-Birth-Acceptor: Easily-Synthesized Mixture for Easily-Fabricated Quaternary Organic Solar Cells with Beyond 20% Efficiency. Angew Chem Int Ed Engl. 2025:e202515114.
4. Luke J, Yang EJ, Labanti C, Park SY, Kim JS. Key molecular perspectives for high stability in organic photovoltaics. Nature Reviews Materials. 2023;8(12):839-52.
5. Ding P, Yang D, Yang S, Ge Z. Stability of organic solar cells: toward commercial applications. Chem Soc Rev. 2024;53(5):2350-87.
6. Wu MH, Ma B, Li SS, Han JQ, Zhao WC. Powering the Future: A Critical Review of Research Progress in Enhancing Stability of High-Efficiency Organic Solar Cells. Adv Funct Mater. 2023;33(50).
7. Luke J, Speller EM, Wadsworth A, Wyatt MF, Dimitrov S, Lee HKH, et al. Twist and Degrade-Impact of Molecular Structure on the Photostability of Nonfullerene Acceptors and Their Photovoltaic Blends. Advanced Energy Materials. 2019;9(15).
8. Luke J, Yang EJ, Chin YC, Che YX, Winkler L, Whatling D, et al. Strong Intermolecular Interactions Induced by High Quadrupole Moments Enable Excellent Photostability of Non-Fullerene Acceptors for Organic Photovoltaics. Advanced Energy Materials. 2022;12(30).
9. Wang YW, Luke J, Privitera A, Rolland N, Labanti C, Londi G, et al. The critical role of the donor polymer in the stability of high-performance non-fullerene acceptor organic solar cells. Joule. 2023;7(4):810-29.
10. Clarke AJ, Luke J, Meitzner R, Wu JY, Wang YM, Lee HKH, et al. Non-fullerene acceptor photostability and its impact on organic solar cell lifetime. Cell Reports Physical Science. 2021;2(7).

View Article Online
DOI: 10.1039/D5EL00166H

11. Planes E, Juillard S, Matheron M, Charvin N, Cros S, Qian DP, et al. Encapsulation Effect on Performance and Stability of Organic Solar Cells. Advanced Materials Interfaces. 2020;7(15).
12. Adams J, Salvador M, Lucera L, Langner S, Spyropoulos GD, Fecher FW, et al. Water Ingress in Encapsulated Inverted Organic Solar Cells: Correlating Infrared Imaging and Photovoltaic Performance. Advanced Energy Materials. 2015;5(20).
13. Viswanathan VN, Ferguson AJ, Pfeilsticker JR, Larson BW, Garner LE, Brook CP, et al. Strategic fluorination of polymers and fullerenes improves photostability of organic photovoltaic blends. Org Electron. 2018;62:685-94.
14. Speller EM, Clarke AJ, Aristidou N, Wyatt MF, Francas L, Fish G, et al. Toward Improved Environmental Stability of Polymer:Fullerene and Polymer:Nonfullerene Organic Solar Cells: A Common Energetic Origin of Light- and Oxygen-Induced Degradation. ACS Energy Lett. 2019;4(4):846-52.
15. Hodsden T, Thorley KJ, Panidi J, Basu A, Marsh AV, Dai HJ, et al. Core Fluorination Enhances Solubility and Ambient Stability of an IDT-Based n-Type Semiconductor in Transistor Devices. Adv Funct Mater. 2020;30(17).
16. Thorley KJ, McCulloch I. Why are S–F and S–O non-covalent interactions stabilising? Journal of Materials Chemistry C. 2018;6(45):12413-21.
17. Boufflet P, Han Y, Fei Z, Treat ND, Li R, Smilgies DM, et al. Using Molecular Design to Increase Hole Transport: Backbone Fluorination in the Benchmark Material Poly(2,5-bis(3-alkylthiophen-2-yl)thieno[3,2-b]-thiophene (pBTTT). Adv Funct Mater. 2015;25(45):7038-48.
18. Li W, Albrecht S, Yang L, Roland S, Tumbleston JR, McAfee T, et al. Mobility-controlled performance of thick solar cells based on fluorinated copolymers. J Am Chem Soc. 2014;136(44):15566-76.
19. Xu T, Yu L. How to design low bandgap polymers for highly efficient organic solar cells. Mater Today. 2014;17(1):11-5.
20. Dai T, Meng Y, Wang Z, Lu J, Zheng Z, Du M, et al. Modulation of Molecular Quadrupole Moments by Phenyl Side-Chain Fluorination for High-Voltage and High-Performance Organic Solar Cells. J Am Chem Soc. 2025;147(5):4631-42.
21. Li ZD, Zhang T, Xin Y, Zhao XL, Yang DL, Wu F, et al. Synergistic effect of fluorination and regio-regularity on the long-term thermal stability of polymer solar cells. Journal of Materials Chemistry A. 2016;4(47):18598-606.
22. Hu Z, Haws RT, Fei Z, Boufflet P, Heeney M, Rossky PJ, et al. Impact of backbone fluorination on nanoscale morphology and excitonic coupling in polythiophenes. Proc Natl Acad Sci U S A. 2017;114(20):5113-8.
23. Son HJ, Wang W, Xu T, Liang YY, Wu YE, Li G, et al. Synthesis of Fluorinated Polythienothiophene-benzodithiophenes and Effect of Fluorination on the Photovoltaic Properties. Journal of the American Chemical Society. 2011;133(6):1885-94.
24. Yang L, Tumbleston JR, Zhou H, Ade H, You W. Disentangling the impact of side chains and fluorine substituents of conjugated donor polymers on the performance of photovoltaic blends. Energy Environ Sci. 2013;6(1):316-26.
25. Ye L, Jiao X, Zhou M, Zhang S, Yao H, Zhao W, et al. Manipulating aggregation and molecular orientation in all-polymer photovoltaic cells. Adv Mater. 2015;27(39):6046-54.
26. Zheng Z, Yao H, Ye L, Xu Y, Zhang S, Hou J. PBDB-T and its derivatives: A family of polymer donors enables over 17% efficiency in organic photovoltaics. Mater Today. 2020;35:115-30.
27. Zhang M, Guo X, Ma W, Ade H, Hou J. A Large-Bandgap Conjugated Polymer for Versatile Photovoltaic Applications with High Performance. Adv Mater. 2015;27(31):4655-60.

View Article Online
DOI: 10.1039/D5EL00166H

28. Prasad S, Genene Z, Marchiori CFN, Singh S, Ericsson LKE, Wang E, et al. Effect of molecular structure on the photochemical stability of acceptor and donor polymers used in organic solar cells. Materials Advances. 2024;5(19):7708-20.
29. Fei Z, Eisner FD, Jiao X, Azzouzi M, Rohr JA, Han Y, et al. An Alkylated Indacenodithieno[3,2-b]thiophene-Based Nonfullerene Acceptor with High Crystallinity Exhibiting Single Junction Solar Cell Efficiencies Greater than 13% with Low Voltage Losses. Adv Mater. 2018;30(8).
30. Eisner FD, Azzouzi M, Fei Z, Hou X, Anthopoulos TD, Dennis TJS, et al. Hybridization of Local Exciton and Charge-Transfer States Reduces Nonradiative Voltage Losses in Organic Solar Cells. J Am Chem Soc. 2019;141(15):6362-74.
31. Zheng XM, Lu H, Feng SY, Hou R, Liu WL, Ming SL, et al. Effect of polymer molecular weight and processing solvent on the morphology and photovoltaic performance of inverted non-fullerene solar cells. Dyes and Pigments. 2021;194.
32. Liu Q, Fang J, Wu J, Zhu L, Guo X, Liu F, et al. Tuning Aggregation Behavior of Polymer Donor viaMolecular-Weight Control for Achieving 17.1% Efficiency Inverted Polymer Solar Cells. Chin J Chem 2021;39(7):1941-7.
33. Qian DP, Ye L, Zhang MJ, Liang YR, Li LJ, Huang Y, et al. Design, Application, and Morphology Study of a New Photovoltaic Polymer with Strong Aggregation in Solution State. Macromolecules. 2012;45(24):9611-7.
34. Chin YC, Daboczi M, Henderson C, Luke J, Kim JS. Suppressing PEDOT:PSS Doping-Induced Interfacial Recombination Loss in Perovskite Solar Cells. ACS Energy Letters. 2022;7(2):560-8.
35. Fu Y, Lee TH, Chin YC, Pacalaj RA, Labanti C, Park SY, et al. Molecular orientation-dependent energetic shifts in solution-processed non-fullerene acceptors and their impact on organic photovoltaic performance. Nat Commun. 2023;14(1):1870.
36. Hou J, Inganas O, Friend RH, Gao F. Organic solar cells based on non-fullerene acceptors. Nat Mater. 2018;17(2):119-28.
37. Speller EM, Clarke AJ, Luke J, Lee HKH, Durrant JR, Li N, et al. From fullerene acceptors to non-fullerene acceptors: prospects and challenges in the stability of organic solar cells. Journal of Materials Chemistry A. 2019;7(41):23361-77.
38. Daboczi M, Hamilton I, Xu S, Luke J, Limbu S, Lee J, et al. Origin of Open-Circuit Voltage Losses in Perovskite Solar Cells Investigated by Surface Photovoltage Measurement. ACS Appl Mater Interfaces. 2019;11(50):46808-17.
39. Lee S, Kim DB, Hamilton I, Daboczi M, Nam YS, Lee BR, et al. Control of Interface Defects for Efficient and Stable Quasi-2D Perovskite Light-Emitting Diodes Using Nickel Oxide Hole Injection Layer. Adv Sci (Weinh). 2018;5(11):1801350.
40. Yang EJ, Luke J, Fu Y, Qiao ZR, Bidwell M, Marsh AV, et al. Unraveling the Impact of Solution Filtration on Organic Solar Cell Stability. Adv Funct Mater. 2024;34(42).
41. Anderson MA, Hamstra A, Larson BW, Ratcliff EL. Distinguishing photo-induced oxygen attack on alkyl chain conjugated backbone for alkylthienyl-benzodithiophene (BDTT)-based push-pull polymers. Journal of Materials Chemistry A. 2023;11(33):17858-71.
42. Frisch MJ, Trucks GW, Schlegel HB, Scuseria GE, Robb MA, Cheeseman JR, et al. Gaussian 16 Rev. C.01. Wallingford, CT2016.
43. Grossman EF, Daramola DA, Botte GG. Comparing B3LYP and B97 Dispersion-corrected Functionals for Studying Adsorption and Vibrational Spectra in Nitrogen Reduction. ChemistryOpen. 2021;10(3):316-26.
44. Becke AD. Density-functional thermochemistry. III. The role of exact exchange. The Journal of Chemical Physics. 1993;98(7):5648-52.

View Article Online
DOI: 10.1039/D5EL00166H

45. Stephens PJ, Devlin FJ, Chabalowski CF, Frisch MJ. Ab-Initio Calculation of Vibrational Absorption and Circular-Dichroism Spectra Using Density-Functional Force-Fields. J Phys Chem. 1994;98(45):11623-7.
46. Breneman CM, Wiberg KB. Determining Atom-Centered Monopoles from Molecular Electrostatic Potentials - the Need for High Sampling Density in Formamide Conformational-Analysis. J Comput Chem. 1990;11(3):361-73.
47. Xu H, Han JH, Babics M, Huerta Hernandez L, Rosas Villalva D, Sanviti M, et al. Elucidating the photodegradation pathways of polymer donors for organic solar cells with seven months of outdoor operational stability. Nat Photonics. 2025;19(4):415-+.
48. Lu T, Chen FW. Bond Order Analysis Based on the Laplacian of Electron Density in Fuzzy Overlap Space. J Phys Chem A. 2013;117(14):3100-8.
49. Ilan YA, Czapski G, Meisel D. The one-electron transfer redox potentials of free radicals. I. The oxygen/superoxide system. Biochim Biophys Acta. 1976;430(2):209-24.
50. Kim S, Rashid MA, Ko T, Ahn K, Shin Y, Nah S, et al. New Insights into the Photodegradation Mechanism of the PTB7-Th Film: Photooxidation of π-Conjugated Backbone upon Sunlight Illumination. J Phys Chem C. 2020;124(5):2762-70.
51. Ashfold MNR, Bain M, Hansen CS, Ingle RA, Karsili TNV, Marchetti B, et al. Exploring the Dynamics of the Photoinduced Ring-Opening of Heterocyclic Molecules. J Phys Chem Lett. 2017;8(14):3440-51.
52. Che Y, Niazi MR, Izquierdo R, Perepichka DF. Mechanism of the Photodegradation of A-D-A Acceptors for Organic Photovoltaics*. Angew Chem Int Ed Engl. 2021;60(47):24833-7.

View Article Online
DOI: 10.1039/D5EL00166H

Data for this article, comprising all the data used to make the figures in the article and supporting information, as well as the Gaussian output files from simulations, are available at the Open Science Framework at https://osf.io/e9wjn/. The project will be made public upon acceptance for publication.